Chemical Physics Letters 883 (2026) 142513

Contents lists available at ScienceDirect

Chemical Physics Letters

journal homepage: www.elsevier.com/locate/cplett

Research paper

Single molecule thermal gearing effect

Piyush Kanti Sarkar [a,*], Soyoung Park [b,c], Kedar Sharma [a], Ningwei Sun [b,c], Franziska S.-C. Lissel [b,c], Christian Joachim [a,*]

[a] Centre d'Élaboration de Matériaux et d'Études Structurales (CEMES), Centre National de la Recherche Scientifique (CNRS-UPR 8011), 29 Rue J. Marvig, BP 94347, 31055 Toulouse Cedex, France
[b] Leibniz Institute of Polymer Research (IPF Dresden), Hohe Strasse 6, 01069 Dresden, Germany
[c] Institute for Applied Polymer Physics, TU Hamburg, 21073 Hamburg, Germany

HIGHLIGHTS

- Soft rotational mechanical manipulation of a single molecule with STM-tip at LN_2.
- Thermally activated gearing effect between two HBDC molecules on an Au(111) surface.
- Dynamic analysis of thermal gearing using coupled Langevin equations.

GRAPHICAL ABSTRACT

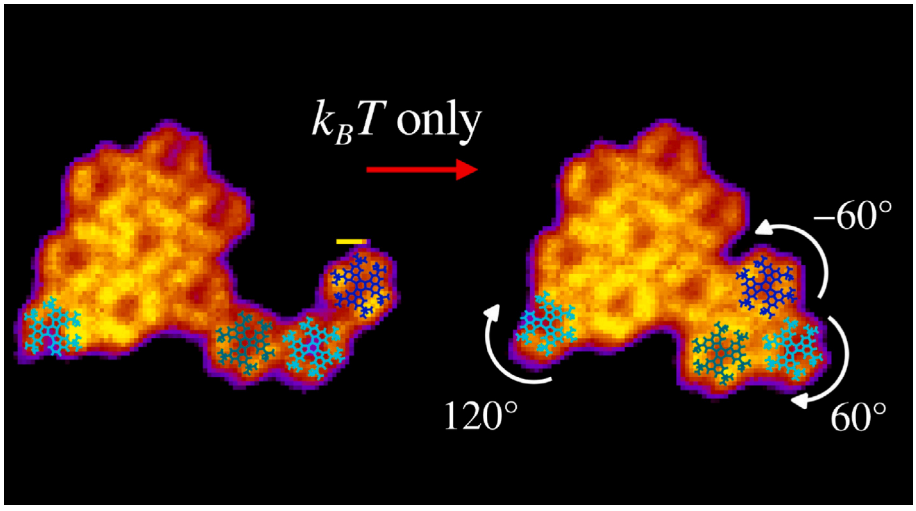

ARTICLE INFO

Keywords:
STM
HBDC
Thermal-rotation
Molecule-gear

ABSTRACT

Observation of a thermally activated gearing effect between two hexa-*tert*-butyl-decacyclene (HBDC) molecule-gears is reported using the Au(111) surface to constrain lateral diffusion of the molecules at 77 K. An on-purpose selected small 2D HBDC nano-island is first destabilized using the tip of a scanning tunneling microscope (STM) in a soft-pulling mode of molecular manipulation. It follows a long sequence of thermally activated spontaneous molecular reconfigurations, leading up to a molecular gearing effect. Using coupled Langevin equations, a simulation of this thermal process is proposed to determine the conditions for this thermally activated gearing effect.

* Corresponding authors.
E-mail addresses: piyush.sarkar@cemes.fr (P.K. Sarkar), christian.joachim@cemes.fr (C. Joachim).

https://doi.org/10.1016/j.cplett.2025.142513
Received 28 July 2025; Received in revised form 9 September 2025; Accepted 3 November 2025
Available online 5 November 2025

1. Introduction

In a 2D domain within a structured molecular monolayer, the first evidence of a thermally activated molecular gearing effect was reported in 1986, through comparative studies of the orientations of the PF_3 and NH_3 monolayer domain adsorbed on a metallic surface [1,2]. On a surface, an intermolecular mechanical gearing effect was obtained using a low temperature ultra-high vacuum scanning tunneling (LT-UHV STM) to construct a molecular rack & pinion machinery [3]. This classical gearing was activated by mechanical push with an STM tip to the pinion molecule moving along the molecular track [3]. Later, an intermolecular gearing effect between the molecules was observed by the construction of a train of molecule-gears [4,5]. A rotation of the first gear of the train, mechanically activated by the STM tip, propagates along the train in a semi-classical mechanical manner [6] almost like a micron-scale solid-state gear train [7,8]. The first attempt to observe a thermally driven gearing effect between two molecules without mechanical interaction from the STM tip was conducted by the H. Gao group [9]. At 77 K, driven solely by thermal energy from the substrate, a tetra-*tert*-butyl zinc phthalocyanine ((*t*-Bu)$_4$-ZnPc) molecule mounted on a single gold adatom rotates randomly as expected. However, when a second (*t*-Bu)$_4$-ZnPc molecule is positioned to mechanically engage with the first one, using STM manipulation, the mutual rotation of the two is blocked. Driven by the surface heat, the motive power of the first (*t*-Bu)$_4$-ZnPc is not enough to drive the rotation of the second one (or the reverse).

In this article, we report the observation of a fully thermally activated intermolecular gearing effect between two hexa-*tert*-butyldecacyclene (HBDC) molecule-gears. Understanding how the thermal heat captured by one molecule on a surface can drive the rotation of a second nearby molecule is of prime importance to explain the emergence of domain orientations during the formation of 2D monolayers of rotating molecules [1]. It also helps to understand how the initial rotation of only one molecule can propagate coherently in a 2D assembly of molecule-rotors [10] and to experimentally approach the concept of a mono-thermal quantum molecule motor [11]. To explore this phenomenon, we used an Au(111) surface with its well-known herringbone reconstruction, which provides confinement of adsorbed HBDC molecules at low temperatures, guiding their lateral diffusion along face-centered cubic (fcc) tracks.

Section 2 describes the preparation of the Au(111) surface, the synthesis of HBDC molecules, the sub-monolayer deposition process, and the STM imaging conditions used to observe thermally activated rotation and diffusion of single molecule along an fcc track of the Au(111) reconstructed surface. Section 3 presents a molecular manipulation experiment in which a single HBDC molecule in a nano-island is rotated by 60° using an STM manipulation in soft constant-current pulling mode, while a nearby molecule of the same island continues to rotate randomly and independently. In Section 4, following the mechanical destabilization of a carefully selected small HBDC nano-island, we describe the spontaneous time sequence of thermally activated molecular events leading to a single-molecule gearing effect. Section 5 provides a discussion of the observed gearing using a simple simulation of this thermal process with coupled Langevin equations, one per gear.

2. Experimental method and set-up

To prepare the experimental conditions for the observation of a thermally activated gearing effect and to avoid long molecule-per-molecule STM manipulation procedures to construct the required molecular experimental machinery, an Au(111) surface was selected. The native herringbone reconstruction of this surface offers fcc tracks which facilitate thermally driven diffusion of single molecules along the surface [12]. The HBDC molecules were selected because of their six-tooth-like van der Waals geometry (see Supp. Info. 1), which is critical for enabling intermolecular mechanical coupling and the gearing effect. When confined within a molecular nanocavity and thermally activated at room temperature (RT) on a Cu(100) surface, a single HBDC molecule rotates randomly [13]. It can also diffuse laterally along this surface at RT if it is not trapped [14].

To achieve a precise molecular behavior between complete freezing (T = 7 K) and excessive thermal motion (at RT), experiments were carried out at T = 77 K (liquid nitrogen temperature, LN_2). This temperature was found to be ideal for the formation of small and stable 2D nano-islands of HBDC molecules at the herringbone kink between adjacent fcc tracks on the Au(111) surface. Working at the LN_2 temperature also minimizes random thermal jumps over the reconstructions, which are known to block single molecule rotations at this temperature [15]. Notice also that the observation of the events of random thermal motion of single molecule requires long sequences of STM imaging at the same location to capture such rare events. To rule out the effect of tip-induced rotation or lateral diffusion (even at low voltage), a long time gap is required in between those scans to allow the thermal activation of such a single event to occur independently of the tip presence. This requires the use of a very stable UHV-STM at 77 K to be able to return to the exact scan area after a long time span, for example, a few days, without scanning this surface location or after scanning at other locations on the surface that are very far away. Although this is a standard performance for the actual LT-UHV STM, working at LN_2 temperature imposes the use of an STM instrument with minimum lateral and vertical drift. Our LT-UHV 4-STM turns out to be an ideal machine for such long-duration experiments (lateral drift values: 0.64 $\mathrm{nm\,h^{-1}}$ at LN_2) due to its large inverted cryostat. Starting at LN_2, the surface temperature can also be increased using a Joule heater available on our LT-UHV 4-STM stage. The results presented below were obtained remaining at LN_2 temperature, as increasing the surface temperature over 77 K triggers a large number of random lateral jumps of HBDCs over the fcc tracks of the Au(111) herringbone reconstructions.

The initial decacyclene and final HBDC molecules were synthesized following procedures reported in the literature [16,17], with modifications as detailed in Suppl. Info. 2. Synthesis protocols were adjusted to optimize yield and purity. The compounds were purified through filtration, column chromatography, and recrystallization, with particular care taken to remove residual low molecular weight species that could otherwise sublimate during subsequent deposition processes. The structural characterization of the purified molecules was conducted using ^{1}H and ^{13}C nuclear magnetic resonance (NMR) spectroscopy (Fig. S2, S3, and S4), as well as electrospray ionization high-resolution mass spectrometry (ESI-HRMS), which confirms the successful synthesis and purity of the target compounds.

Before depositing the molecules on the surface, an Au(111) single crystal was prepared under ultra-high vacuum (UHV) conditions by repeated cycles of Ar^+ ion sputtering (1.0 keV, $\sim 10^{-6}$ mbar, 10 min) followed by annealing at 470 °C for 1 h. Chemical purification procedures were specifically optimized to ensure that no low molecular weight species were present, thus preventing contamination of the Au(111) surface during molecule sublimation. The very sub-monolayer of HBDC molecules was sublimated from a quartz crucible at 260 °C on the UHV-clean-prepared Au(111) surface, which was kept at RT under a base pressure of $\sim 1 \times 10^{-9}$ mbar in the preparation chamber of LT-UHV 4-STM. STM images were recorded using the LT-UHV 4-STM, with the stage maintained at LN_2 temperature to benefit from the occasional movement (diffusion) of HBDC molecules along the fcc track at this temperature, helping to observe the thermal gearing effect. All the STM images were recorded in constant current mode at a moderate bias voltage and under a base pressure of $\sim 4 \times 10^{-11}$ mbar. On the LT-UHV 4-STM, the bias voltage is applied to our electrochemically etched tungsten tips relative to the grounded sample stage. The orientations of the STM tip can be 45° or 90° vertical relative to the Au(111) surface for imaging or manipulation.

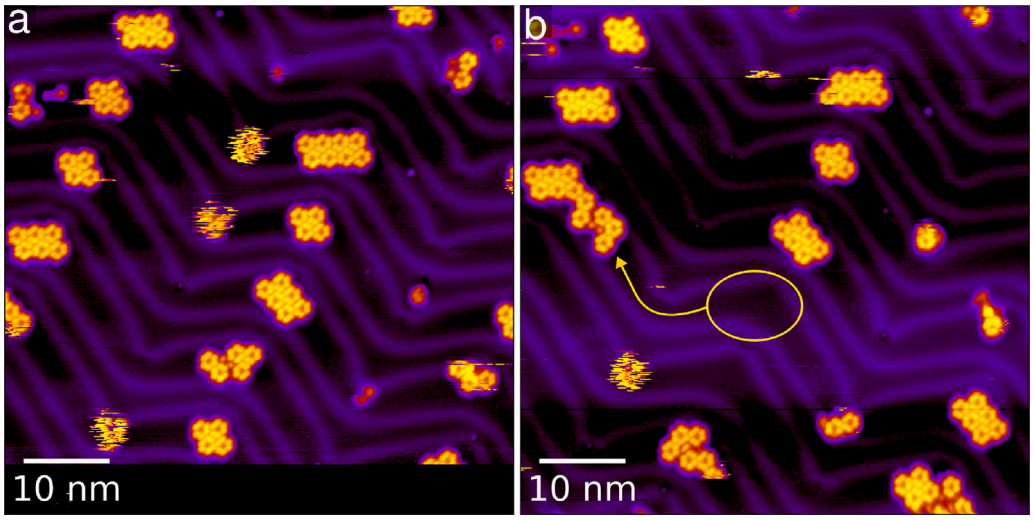

Fig. 1. LT-UHV STM images recorded on the LT-UHV 4-STM at 77 K. (a) First image shows the self-assembly of many small 2D nano-islands stabilized by the native Au(111) herringbone surface reconstruction. (b) Image of the same location recorded 115 min after (a). Multiple spontaneous thermal lateral diffusion of the HBDC islands are observed along the fcc tracks. The one indicated by the yellow circles demonstrates the lateral diffusion and internal re-organization of 6 HBDC molecules along and under the constrain of the Au(111) reconstruction corrugation walls. $I = 10$ pA, $V = -800$ mV.

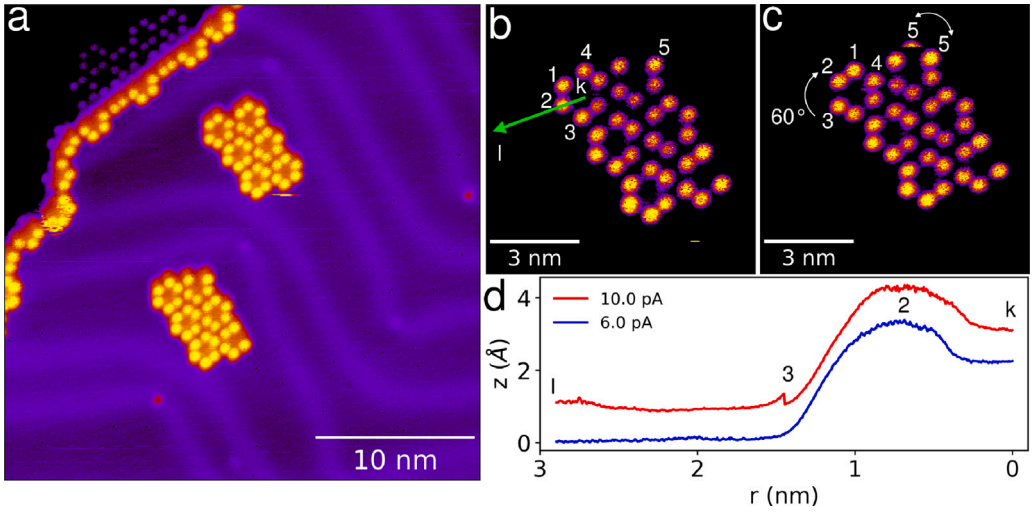

Fig. 2. (a) Image of 2 isolated stable 2D nano-islands comprising 6 HBDC molecules well stabilized in the fcc part on the Au(111) surface reconstruction. (b) STM scan image of one nano-island indicating the teeth positions of the HBDC before performing a mechanical pull line scan with the STM tip. Manipulation is performed exactly along the k to l arrow as indicated. (c) STM scan image recorded after the manipulation with 10 pA of tunneling current. Also observed during the imaging: the destabilization of the top right missing teeth HBDC with its intermediate anti-clockwise rotation during the imaging. (d) The manipulation line scans for two different tunneling current. The pulling jump (3) observed on the red line scan resulted from a 60° clockwise rotation of the scanned HBDC molecule. All images $I = 6$ pA, $V = -600$ mV. The color contrast of the (b) and (c) images have been increased as compared to (a) to follow the HBDC rotations. Interpretation of the observed surface conformation is provided in Supp. Info. 4.

As presented in Fig. 1, a very sub-monolayer of HBDC sublimation leads to many small 2D nano-islands randomly distributed along the fcc tracks with an average of 4 to 8 HBDC molecules per nano-island, mechanically well engaged by their teeth. At LN_2 temperature, some isolated single HBDCs are diffusing along the fcc tracks, producing some jumps from time to time in the tunneling current intensity while scanning. The nano-island, comprising 5 HBDC + 2 trapped impurities (marked with a yellow circle in Fig. 1a), spontaneously diffused to the left along a single fcc track and reached a blocking point (here a 6 HBDC nano-island) as reported in Fig. 1b. This spontaneous motion occurred while scanning at another location on the surface for about 2 h. We have observed many such diffusion examples whose exact timing is not known. During this lateral diffusion, the two corrugation walls (height of ~ 20 pm), which originated due to the densification of Au atoms on the close-packed (111) surface on either side of the fcc track, restricted the 5 HBDC nano-island to remain along the track. This movement ended at a blocking point with the formation of a new flat cluster configuration. This type of fcc track guiding was beneficial for Nanocar race I and II, albeit not thermally activated, since it was performed at 5 K [18]. Detail interpretation of molecular configuration in the initial Fig. 1a and the final Fig. 1b (Suppl. Info. 3, Fig. S5) explains this complex lateral diffusion process, including a thermally activated 60° rotation of an HBDC molecule.

3. Single HBDC molecule rotation: STM manipulation versus thermal activation

To understand the thermally activated reconfiguration processes in a nano-island as presented in Fig. 1 and to determine the reconfiguration process of an HBDC nano-island leading to a thermal gearing effect,

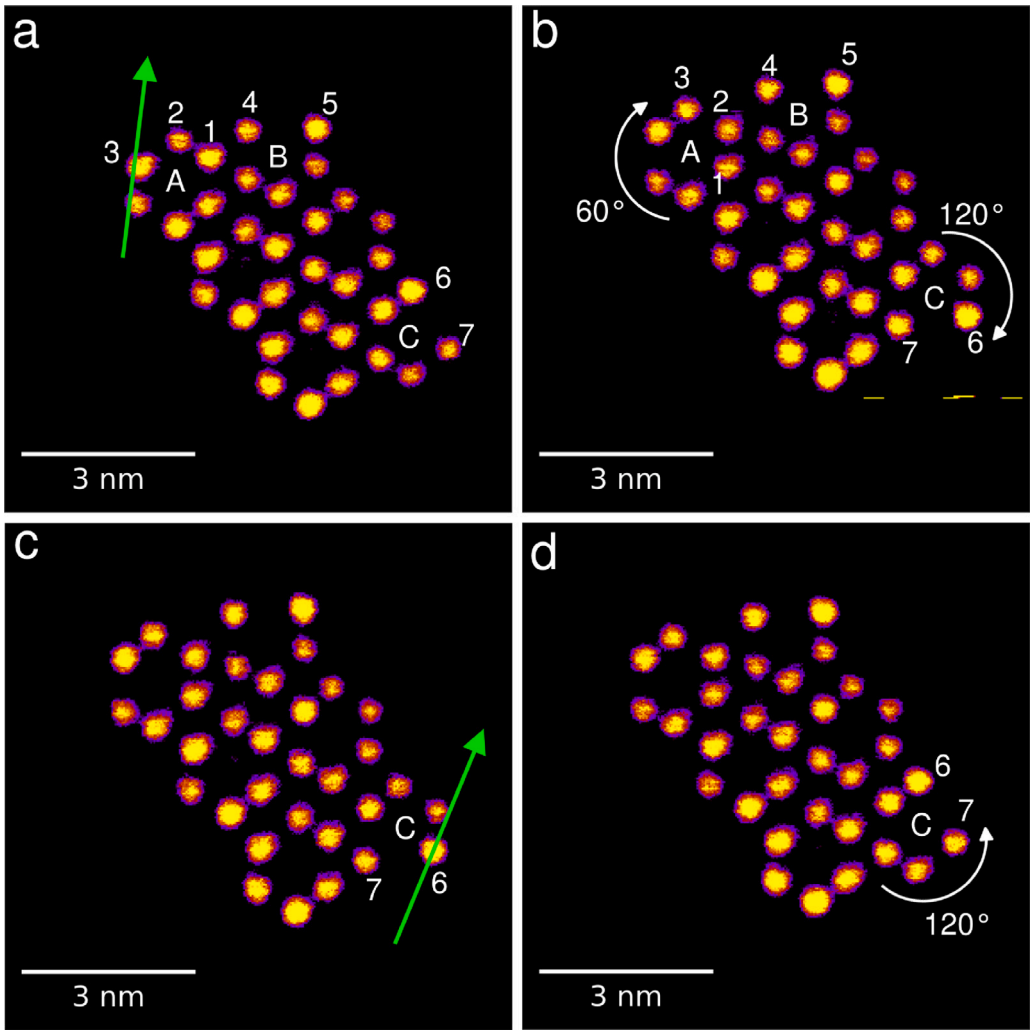

Fig. 3. (a) The HBDC A rotated 60° clockwise in a pushing mode of manipulation with no apparent rotation of HBDC B. (b) An uncorrelated 120° clockwise rotation of HBDC C after pushing on HBDC A. (c) to (d) HBDC C was pushed back in its original orientation with no consequent rotation of HBDC A. Molecular manipulation in a pushing mode performed with the STM feedback set up: $I = 50$ pA, $V = -600$ mV. All STM images were recorded at $I = 6$ pA, $V = -600$ mV.

we compared the rotation of a single HBDC molecule triggered by gentle STM tip manipulation and by thermal energy. For this purpose, we selected a nano-island, comprising six HBDCs, well stabilized by an Au(111) surface reconstruction kink in between the fcc linear tracks (Fig. 2a). In addition, one missing-tooth HBDC molecule acted as a tag to follow a single HBDC molecular rotation event. Another criterion to select the given HBDC nano-island was to enable the tip apex-end atom to access any of the HBDC molecules for mechanical manipulation in a given nano-island, which limited the width of a nano-island to 2 HBDC molecules. Mechanical manipulation with the STM tip was employed in constant current pulling mode to minimize the mechanical interaction between the apex of the tip end and the selected HBDC. The manipulation pulling threshold was determined by gradually increasing the STM feedback current, starting from a value where no movement was observed. The feedback loop signal was time recorded (Δz vs. time) at each line scan, then converted to a scan length (Δz vs. distance) [19]. As presented in Fig. 2d, such a line scan is very stable up to a current threshold where the Δz jump (3) occurs during a mechanical pull along the line. This Δz jump indicates that one HBDC had moved laterally during this line scan. This molecular manipulation was performed on the bottom nano-island of Fig. 2a comprising 6 HBDC molecules. After zooming on it, the STM tip apex was positioned at the center k of a lateral HBDC and line scans were performed from k to l, for different incremental tunneling currents. The teeth positions of the concerned molecule, before and after the line scan, are indicated in Figs. 2b and 2c, respectively (see also Suppl. Info. 4). The threshold for pulling manipulation is reached at $I = 10$ pA ($R_t = 60$ GΩ) leading to the Δz small jump (3) along the scan line to compensate for the increase in tunnel current resulting from the 60° rotation of the HBDC molecule during this scan. The STM image after this manipulation shows (Fig. 2c) that this HBDC rotated 60° clockwise because tooth no. 3 was pulled by the tip apex.

At the same time, another HBDC molecule oscillated 60° which can be seen from the double image of the tooth (marked 5) in Fig. 2c. To understand whether this was a fortuitous thermally activated event or a rotation resulting from a gearing effect due to the tip pulling the nearby HBDC, the same manipulation was performed again on HBDC A belonging to the same nano-island (Fig. 3a). This time, HBDC B remained stable during the STM manipulation (Fig. 3b) while HBDC C rotated 120° (noticeable due to its missing tooth). To ensure that it was a thermally activated event, HBDC C was then manipulated back 120° to its original orientation by the tip (Fig. 3c) with no consequence on HBDC A and HBDC B (Fig. 3d). This confirms that the rotation of HBDC C was a thermal event, not correlated with the STM manipulation of HBDC A.

To observe the thermally activated random rotation of a single HBDC at the border of a nano-island, a new nano-island consisting of 8 HBDC molecules was selected with a very specific surface arrangement

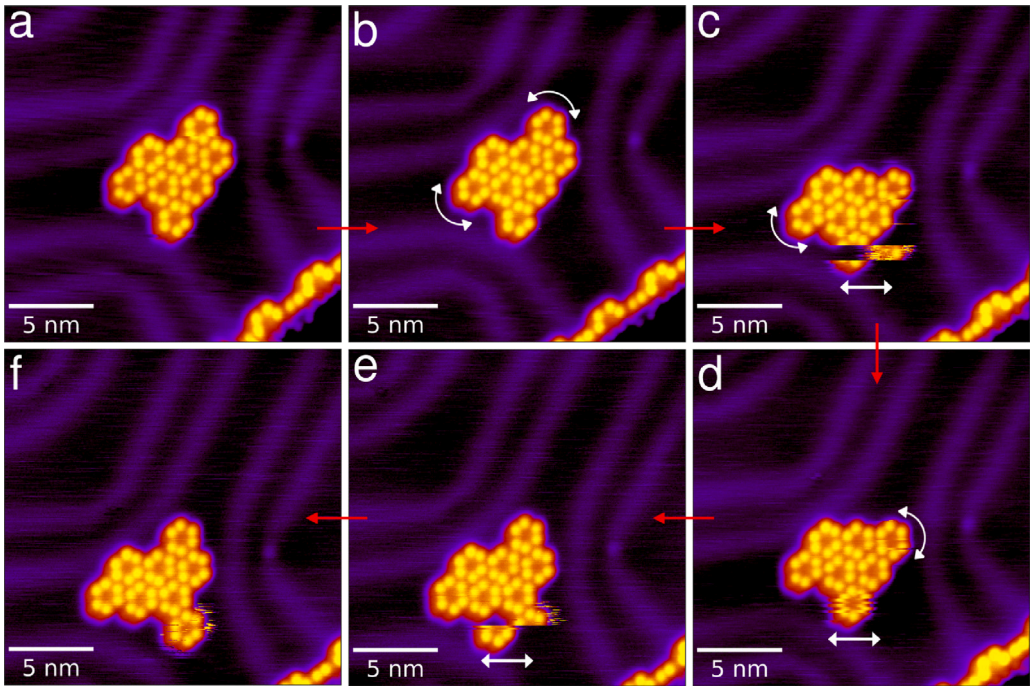

Fig. 4. Spontaneous uncorrelated thermal motion/rotation of HBDC at the edge of an 8 HBDC molecular cluster trapped at a crossing between 3 fcc tracks of the Au(111) surface. At the edge, 3 HBDC are not totally engaged with the other HBDC. (a–b) random rotation of the two external HBDC at the edge of the cluster. (c–d) One HBDC from the upper side moved away from the cluster leaving little space for another HBDC below it to rotate. (e) The missing HBDC joined again at the same position of the cluster. (e to f) the bottom HBDC is trying to sit to another available position at the edge and its going back and forth between these two accessible positions. One image recording time: 11 min. No time laps between 2 images. All STM images recorded at $I = 6$ pA, $V = -500$ mV.

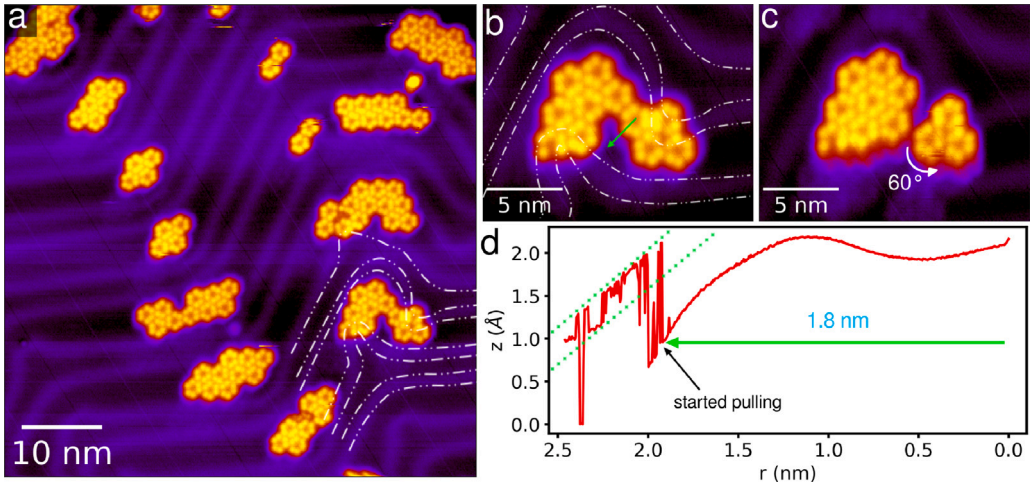

Fig. 5. (a) STM scan image at another location as compared with Fig. 1. The bottom-right cluster of 11 HBDC is selected for further experiment. The cluster is constrained in between the Au(111) herringbone reconstruction i.e. stable enough over time against lateral thermal activated diffusion at 77 K. (b) Zoomed image of the cluster with the marked Au(111) reconstruction lines and the STM tip trajectory (green arrow) for single HBDC STM manipulation in a pulling mode. (c) Image of the HBDC molecules nano-island after this STM manipulation. (d) The recorded manipulation signal demonstrating how at constant current the tip apex is passing over the HBDC for 1.8 nm (i.e 30 s) and then is pulling the HBDC molecule.

(Fig. 4a). Here, only 2 to 3 HBDC molecules sitting at the border of the nano-island are potentially free to rotate, being located at an open space fcc track with no constrain. We have performed many scans on this new Fig. 4a nano-island waiting for a single thermally activated HBDC rotation event, with a suitable STM feedback parameters to avoid any tip-induced mechanical manipulation. Those scan sequences are presented in Fig. 4. The HBDC located at the left end rotates by 60° from time to time, while another one located at the top-right end disappeared away (Fig. 4c), diffusing along its fcc track. The surface thermal energy is enough to drive one or a few HBDCs to trigger a non-directional rotation or a motion along an fcc track (sequence from Figs. 4d to 4f). Notice also that when the top right HBDC returns back (after being missing from Fig. 4c), it recovers its initial docking orientation in its nano-island (Fig. 4e).

4. Thermally activated gearing effect

To observe a thermal activated gearing effect, we selected a different HBDC nano-island more constrained at its borders. Fig. 5 shows that the new selected nano-island, comprising 11 HBDCs, is tightly constrained at its top right end and with only two possible escape

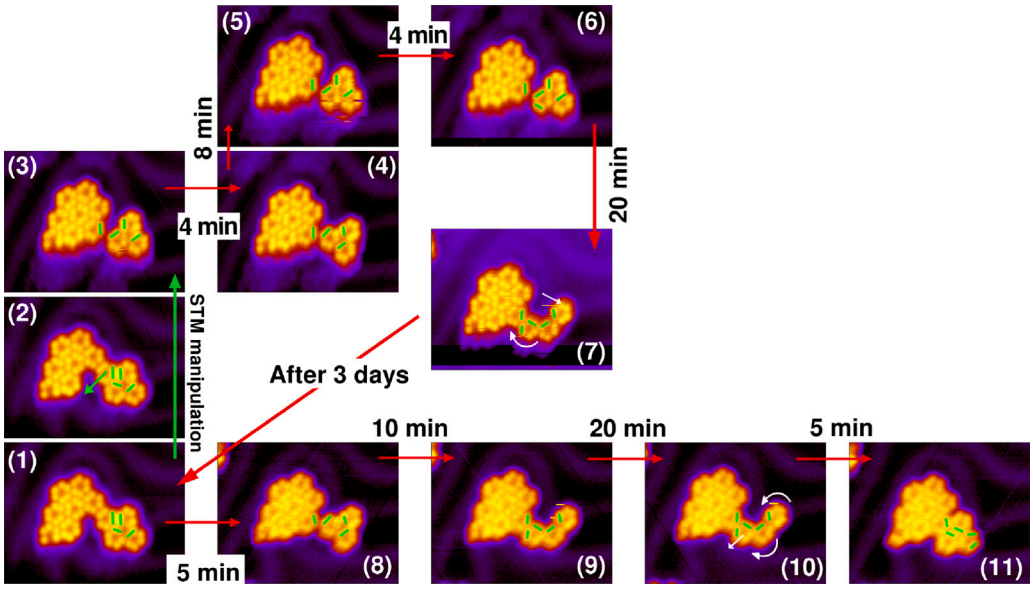

Fig. 6. After the HBDC manipulation in a pulling mode from (1) to (3) as described in Fig. 5, a sequence of constant current STM images on the same Au(111) surface location observing the thermal destabilization of the 11 HBDC cluster imaged in (1). (3) the new 11 HBDC intra-cluster ordering. This thermally unstable (3) then undergoes a succession of spontaneous 60° rotation from (4) to (6) before reaching a new configuration (7) with a train of 3 molecule-gears. Waiting long enough, (7) again recovers its initial configuration (1) spontaneously. But this time, (1) is no more stable at 77 K and reaches (9) similar to (7). It stays in this configuration for another 20 min as shown in (10). Then a spontaneous molecular gearing effect occurs at 77 K to reach (11) (see Fig. 7 for a detail interpretation of this molecular gearing effect). Aside from (2) to (3), STM scanning conditions were chosen in such a way not to perturb the position and conformation of each HBDC. The observed time sequence of the events from (3) to (11) varies from case to case.

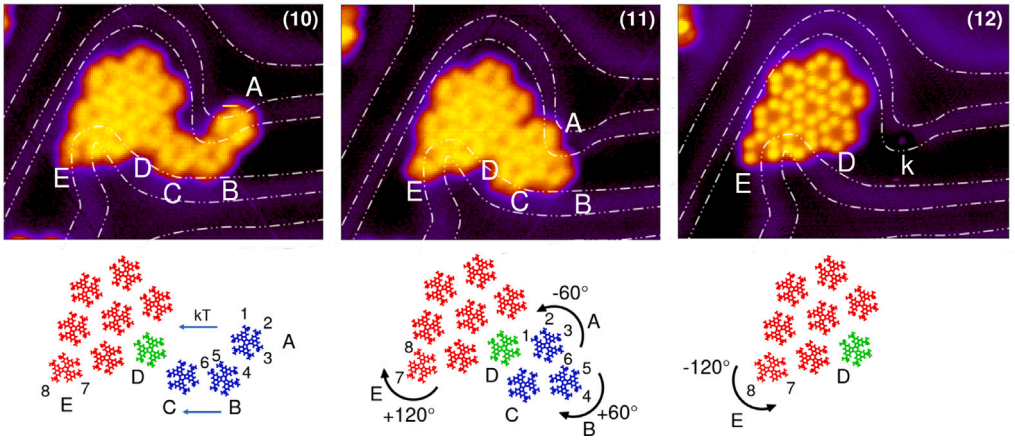

Fig. 7. A detail interpretation of the HBDC molecular conformation in the STM images when spontaneously going from (10) to (11) and ending in (12) without any STM manipulation. The Au(111) surface reconstruction locations is indicated by the white dashed line. From (10) to (11), HBDC E rotates spontaneously 120° clockwise as observed many times like in Figs. 2 and 3. The missing terbutyl tooth acts as tagging to follow the rotation. HBDC A diffuses thermally left rotating 60° anti clockwise. As a consequence, HBDC B rotates 60° clockwise. (12) After waiting for 2 h without scanning, HBDC (A,B,C) moved to the right, diffusing along the fcc track and HBDC E rotated back to initial position. The defect kink "k" can now be imaged after HBDC (A,B,C) left.

routes for the HBDC at the border. Its bottom-left HBDC (Fig. 5b) has one missing tooth which helps to follow possible thermally activated random rotation events. The configuration of this nano-island was quite stable under multiple STM scannings with the bottom-left HBDC rotating from time to time. To mechanically destabilize this nano-island, we performed a single STM manipulation along the arrow as shown in Fig. 5b leading to a new configuration (Fig. 5c) (see Suppl. Info. 5). The manipulation signal is presented in Fig. 5d. This configuration of the nano-island as presented in Fig. 5c is unstable under thermal activation and is now looking for stabilization as indicated in Fig. 6. This stabilization takes around 30 min to achieve the configuration of Fig. 6(7). Surprisingly, after a few days without scanning, Fig. 6(7) recovers its initial Fig. 6(1) configuration activated only by thermal energy. The only difference is that this Fig. 6(7) configuration can again transform to Fig. 6(8) spontaneously with apparently the same intramolecular configuration as that of Fig. 6(3) nano-island. It was not possible here to determine some possible intermediate intramolecular conformation changes. But in any case, Fig. 6(8) can now thermally reach Fig. 6(9) which ends in the Fig. 6(11) configuration after a thermal gearing effect.

To analyze the observed thermal gearing effect from Fig. 6(10) to Fig. 6(11), the exact molecular arrangement of HBDC in the nano-island was decomposed in detail and presented in Fig. 7. Fig. 7(11) is the immediate next scan after Fig. 7(10) with ~ 5 min of STM image recording duration. The change in molecular configuration (presented just below the corresponding STM images in Fig. 7) from Fig. 7(10) to Fig. 7(11), can have two possible interpretations, both thermally activated: (i) HBDC A is thermally diffusing 2.6 nm towards the left,

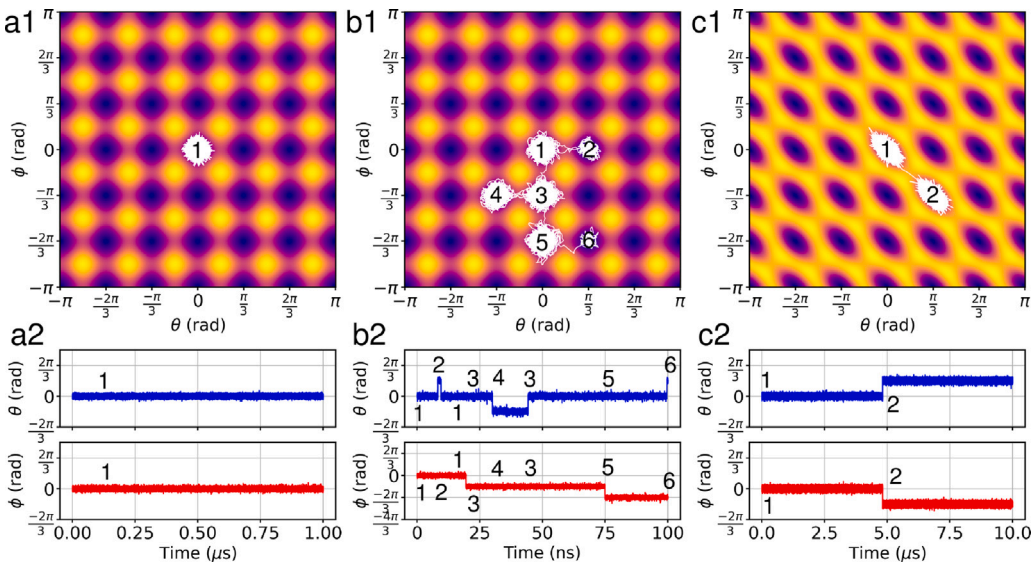

Fig. 8. Simulations of the thermal gearing effect reported in Fig. 7 using a simple mechanical system of two coupled Langevin equations (see Supp. Info 6). For each HBDC, the 50 meV rotation barrier height was chosen for a given gear to rotate 60° in average at 80 K. (a1), (b1), and (c1) are the 2D contour plot of the ground state potential energy surfaces (PES) used in the Langevin with the obtained trajectories super imposed in white. (a2), (b2), and (c2) are the time dependent variations of the rotation angles θ and ϕ calculated by solving the Langevin. For (a1) and (a2), $T = 50$ K is not high enough to provide enough energy to rotate. (b2) a detail interpretation of this random walk on the PES at 80 K for non-engaged state ($k = 0$ meV). Different trials will provide different trajectories. Calculation is limited here to 100 ns not to explore all the presented minima (blue in PES). (c1) The PES is changed due to added interaction potential for $k = 30$ meV. (c2) The trajectory for $k = 30$ meV. For the presented trial, only one gearing event is obtained even after 10 μs of simulation. (Details of the gears structural parameters given in Suppl. Info. 8).

rotating 60° anticlockwise to avoid the Au(111) reconstruction wall. The consequence is a clockwise rotation of HBDC B, resulting also in a left and 0.9 nm downward shift of HBDC C. (ii) First, HBDC B rotates clockwise, forcing HBDC A to rotate 60° anticlockwise and move to the left side under this push. As a consequence, HBDC C also moves to the left. In both cases, HBDC D is not moving and HBDC E rotated 120° clockwise. This last motion is normally independent of the HBDC A, B, & C motions as discussed above. Following observations in [9] that at 77 K a thermal motive power is not strong enough for the mutual rotation of two molecules, we privilege interpretation (i), showing that the thermally activated lateral motion of HBDC A to the left can trigger a single molecule gearing effect, activating the 60° clockwise one-step rotation of HBDC B and the consequent motion of HBDC C to the left. The initial position of HBDC A atop the herringbone reconstruction kink (see also Fig. 7(12)) is unstable according to the thermally activated path between Fig. 6(3) and Fig. 6(6). So, in this interpretation, there is no need to invoke a possible motive power of HBDC B. HBDC B is simply mechanically following the thermally activated instability of HBDC A which needed to rotate anticlockwise to get out of the reconstruction kink. This thermally activated gearing effect cannot go further because of the compact arrangement of the final molecular configuration in Fig. 7(11) (see conformation analysis in Suppl. Info. 6). We waited for some consecutive scans anticipating the detachment of HBDC B, diffusing along its corresponding fcc track as reported in Fig. 4 from Fig. 4b to Fig. 4c. However, about 120 min after the recording of Fig. 7(11), we observed the disappearance of (A, B, C) from the nano-island confirming the stability of the 2D configuration of this 3-HBDC cluster, which is able to diffuse like a single molecular object along the fcc track. Notice that from time to time, this (A, B, C) cluster is shuffling back and forth trying to fit in via its interactions with HBDC D. The duration of this 2D shuffling can be as long as 60 min. Note that we have presented the time sequence of one gearing effect out of many others observed at different locations on the surface. Another example for gearing effect is provided in Suppl. Info. 7.

5. Discussion

To reproduce the observed gearing effect with a simple mechanical model, we used a pair of classical Langevin equations, one for each molecule-gear, assuming that thermally activated motions occur in the electronic ground state and follow a classical mechanical motion [20, 21]. As indicated in Suppl. Info. 8, we used a simple 2D potential energy surface (PES) (Fig. S10) for the rotation of two meshed gears with 6 steps (teeth) between a full 360° rotation. The thermal activation is provided by two uncorrelated noises (one for each gear, i.e. one per Langevin equation) respecting the fluctuation–dissipation theorem in each Langevin equation (See Suppl. Info. 8). The momentum of inertia, the barrier height of the rotational potential energy, and the friction coefficients are of the same order of magnitude as that of a small organic molecule rotating on a metallic surface [22]. The equations are coupled with an interaction potential with an interaction factor 'k', with k being zero when there is no interaction between the gears. As presented in Fig. 8a, for non-engaged gears ($k = 0$) and for a surface temperature not high enough to trigger even a one-step 60° rotation per gear, the rotational motions are random for both with very small rotational angle. The classical rotation trajectory remains inside the initial potential well of their PES in the θ and ϕ rotation angle directions (rotation of gear 1 and gear 2 are represented by θ, and ϕ, respectively). Fig. 8a confirms the reliability of the calculation by the coupled Langevin equations solver, which is further confirmed by plotting the Arrhenius curve per gear characterizing the thermally activated rotational process (Fig. S11). With no interaction between the gears (non-engaged state: $k = 0$) and at a higher surface temperature, each gear rotates randomly independently of each other, with the awaited progression in time with a step of 60°, exploring many minima of the PES around the initial angular position (Fig. 8b). This is exactly what was observed, for example, in Fig. 2c or in Fig. 4 sequences.

Now, when the two gears are engaged, the interaction potential meshing the two leads to a gearing effect even if the noises feeding the rotations are uncorrelated. Fig. 8c demonstrates one such event for $k = 30$ meV in a time span of 10 μs. It is exactly what was observed in

Fig. 7. With varying interaction coefficient (k) relative to the rotation barrier U_0 of the gears (see Suppl. Info. 8, Fig. S12) we can estimate the threshold value of k for Fig. 7 case. When $k \ll U_0$, the two gears are not engaged enough and rotate independently, fed by their local noises. For $k \sim U_0$, when one of the two gears starts to rotate by 60° in one direction, the second rotates 60° one step in the opposite direction. After many trials of solving the Langevin coupled equations, no net rotation is observed in a specific direction. For $U_0 = 50$ meV, this transition for a thermally driven simultaneous ($+\theta$, $-\phi$, or vice versa) single rotation event occurs for about $\sim k > 40$ meV. Whereas, for $U_0 = 20$ meV the threshold for k values for this event to occur decreases to ~ 15 meV (Fig. S13).

In conclusion, by working at a surface temperature between the total freezing of mechanical motion and the complete thermodynamical behavior of a 2D molecular gas of HBDC molecules on a surface, we have observed their slow motions. From time to time, an HBDC molecule rotates step by step and sometimes leaves its nano-island. By constraining those two motions with the help of Au(111) surface reconstruction, we have observed a thermally activated gearing effect between 2 HBDC molecules. It demonstrates that such elementary rotational events exist behind the average behavior described by statistical analysis. It describes how domain orientation is set up while forming a 2D monolayer of rotating molecules. It describes how the rotation of one molecule-gear can propagate coherently along a molecular chain of molecule-rotors. It also helps to experimentally approach the concept of mono-thermal storage in fluctuating rotating molecules. It demonstrates the usefulness of a local single heat reservoir to drive a motion at nanoscale for an optimized chemical gear structure.

CRediT authorship contribution statement

Piyush Kanti Sarkar: Writing – review & editing, Writing – original draft, Validation, Methodology, Investigation, Formal analysis, Data curation. **Soyoung Park:** Writing – original draft, Methodology, Investigation, Data curation. **Kedar Sharma:** Methodology, Investigation, Data curation. **Ningwei Sun:** Methodology, Formal analysis, Data curation. **Franziska S.-C. Lissel:** Writing – review & editing, Validation, Supervision, Funding acquisition, Formal analysis. **Christian Joachim:** Writing – review & editing, Writing – original draft, Supervision, Methodology, Funding acquisition, Formal analysis, Conceptualization.

Declaration of competing interest

The authors declare the following financial interests/personal relationships which may be considered as potential competing interests: Christian Joachim reports financial support was provided by European Innovation Council. Franziska S.-C. Lissel reports financial support was provided by European Innovation Council. Franziska S.-C. Lissel reports financial support was provided by DFG, Ingeborg-Gross Foundation. If there are other authors, they declare that they have no known competing financial interests or personal relationships that could have appeared to influence the work reported in this paper.

Acknowledgments

This work was funded by the European Union. However, the views and opinions expressed are those of the authors only and do not necessarily reflect those of the European Union. Neither the European Union nor the granting authority can be held responsible for them. This work has received funding from then European Innovation Council (EIC) under the project: Energy storage in molecules (ESiM) (grant agreement No. 101046364). Funding from the Ingeborg-Gross Foundation, Germany is gratefully acknowledged. Verlet simulations were performed on the CALMIP supercomputer by granted access to the HPC resources under the allocation 2024-P083.

Appendix A. Supplementary data

Supplementary material related to this article can be found online at https://doi.org/10.1016/j.cplett.2025.142513.

Data availability

Data will be made available on request.

References

[1] M.D. Alvey, J.T. Yates, K.J. Uram, The direct observation of hindered rotation of a chemisorbed molecule: Pf_3 on Ni(111), J. Chem. Phys. 87 (12) (1987) 7221–7228, http://dx.doi.org/10.1063/1.453366.
[2] R. Zwanzig, Rotational relaxation in a gear network, J. Chem. Phys. 87 (8) (1987) 4870–4872, http://dx.doi.org/10.1063/1.452798.
[3] F. Chiaravalloti, L. Gross, K.-H. Rieder, S.M. Stojkovic, A. Gourdon, C. Joachim, F. Moresco, A rack-and-pinion device at the molecular scale, Nat. Mater. 6 (2007) 30–33, http://dx.doi.org/10.1038/nmat1802.
[4] W.-H. Soe, S. Srivastava, C. Joachim, Train of single molecule-gears, J. Phys. Chem. Lett. 10 (21) (2019) 6462–6467, http://dx.doi.org/10.1021/acs.jpclett.9b02259.
[5] K.H. Au Yeung, T. Kühne, F. Eisenhut, M. Kleinwächter, Y. Gisbert, R. Robles, N. Lorente, G. Cuniberti, C. Joachim, G. Rapenne, C. Kammerer, F. Moresco, Transmitting stepwise rotation among three molecule-gear on the Au(111) surface, J. Phys. Chem. Lett. 11 (16) (2020) 6892–6899, http://dx.doi.org/10.1021/acs.jpclett.0c01747.
[6] S. Srivastava, W.-H. Soe, C. Joachim, Building and probing small for mechanics, Advances in Atom and Single Molecule Machines, XIII, Springer Cham, 2020, http://dx.doi.org/10.1007/978-3-030-56777-4.
[7] H.-H. Lin, A. Croy, R. Gutierrez, C. Joachim, G. Cuniberti, Mechanical transmission of rotational motion between molecular-scale gears, Phys. Rev. Appl. 13 (2020) 034024, http://dx.doi.org/10.1103/PhysRevApplied.13.034024, URL https://link.aps.org/doi/10.1103/PhysRevApplied.13.034024.
[8] J. Deng, C. Troadec, F. Ample, C. Joachim, Fabrication and manipulation of solid-state SiO_2 nano-gears on a gold surface, Nanotechnology 22 (27) (2011) 275307, http://dx.doi.org/10.1088/0957-4484/22/27/275307.
[9] L. Gao, Q. Liu, Y.Y. Zhang, N. Jiang, H.G. Zhang, Z.H. Cheng, W.F. Qiu, S.X. Du, Y.Q. Liu, W.A. Hofer, H.-J. Gao, Constructing an array of anchored single-molecule rotors on gold surfaces, Phys. Rev. Lett. 101 (2008) 197209, http://dx.doi.org/10.1103/PhysRevLett.101.197209, URL https://link.aps.org/doi/10.1103/PhysRevLett.101.197209.
[10] Y. Zhang, H. Kersell, R. Stefak, J. Echeverria, V. Iancu, U.G.E. Perera, Y. Li, A. Deshpande, K.-F. Braun, C. Joachim, G. Rapenne, S.-W. Hla, Simultaneous and coordinated rotational switching of all molecular rotors in a network, Nat. Nanotechnol. 11 (2016) 706–712, http://dx.doi.org/10.1038/nnano.2016.69.
[11] K.H. Au-Yeung, S. Sarkar, T. Kühne, O. Aiboudi, D.A. Ryndyk, R. Robles, F. Lissel, N. Lorente, C. Joachim, F. Moresco, Thermal with electronic excitation for the unidirectional rotation of a molecule on a surface, J. Phys. Chem. C 127 (34) (2023) 16989–16994, http://dx.doi.org/10.1021/acs.jpcc.3c04990.
[12] G. Rapenne, C. Joachim, The first nanocar race, Nat. Rev. Mater. 2 (2017) 17040, http://dx.doi.org/10.1038/natrevmats.2017.40.
[13] J.K. Gimzewski, C. Joachim, R.R. Schlittler, V. Langlais, H. Tang, I. Johannsen, Rotation of a single molecule within a supramolecular bearing, Science 281 (5376) (1998) 531–533, http://dx.doi.org/10.1126/science.281.5376.531, URL https://www.science.org/doi/abs/10.1126/science.281.5376.531.
[14] G. Pawin, A.Z. Stieg, C. Skibo, M. Grisolia, R.R. Schilittler, V. Langlais, Y. Tateyama, C. Joachim, J.K. Gimzewski, Amplification of conformational effects via *tert*-butyl groups: Hexa-*tert*-butyl decacyclene on Cu(100) at room temperature, Langmuir 29 (24) (2013) 7309–7317, http://dx.doi.org/10.1021/la304634n.
[15] N. Khera, N. Sun, S. Park, P. Das, K.H. Au-Yeung, S. Sarkar, F. Plate, R. Robles, N. Lorente, F.S.-C. Lissel, F. Moresco, *N*-heterocyclic carbene vs. thiophene – chiral adsorption and unidirectional rotation on Au(111), Angew. Chem. Int. Ed. 64 (17) (2025) e202424715, http://dx.doi.org/10.1002/anie.202424715, URL https://onlinelibrary.wiley.com/doi/abs/10.1002/anie.202424715.
[16] A.W. Amick, L.T. Scott, Trisannulated benzene derivatives by acid catalyzed aldol cyclotrimerizations of cyclic ketones. Methodology development and mechanistic insight, J. Org. Chem. 72 (9) (2007) 3412–3418, http://dx.doi.org/10.1021/jo070080q.
[17] T. Kubo, K. Yamamoto, K. Nakasuji, T. Takui, I. Murata, 4,7,11,14,18,21-Hexa-t-butyltribenzodecacyclenyl radical: A six-stage amphoteric redox system, Bull. Chem. Soc. Jpn. 74 (2001) 1999–2009, URL https://api.semanticscholar.org/CorpusID:96684756.
[18] A. Barragán, T. Nicolás-García, K. Lauwaet, A. Sánchez-Grande, J.I. Urgel, J. Björk, E.M. Pérez, D. Écija, Design and manipulation of a minimalistic hydrocarbon nanocar on Au(111), Angew. Chem. Int. Ed. 62 (6) (2023) e202212395, http://dx.doi.org/10.1002/anie.202212395.

[19] F. Moresco, G. Meyer, K.-H. Rieder, H. Tang, A. Gourdon, C. Joachim, Recording intramolecular mechanics during the manipulation of a large molecule, Phys. Rev. Lett. 87 (2001) 088302, http://dx.doi.org/10.1103/PhysRevLett.87.088302, URL https://link.aps.org/doi/10.1103/PhysRevLett.87.088302.

[20] C. Joachim, J.K. Gimzewski, Single molecular rotor at the nanoscale, in: J.-P. Sauvage (Ed.), Molecular Machines and Motors, first ed., in: Structure and Bonding, vol. 99, Springer Berlin, 2001, pp. 1–18, http://dx.doi.org/10.1007/3-540-44421-1.

[21] A. MacKinnon, Quantum gears: a simple mechanical system in the quantum regime, Nanotechnology 13 (5) (2002) 678, http://dx.doi.org/10.1088/0957-4484/13/5/328.

[22] H.-H. Lin, A. Croy, R. Gutierrez, C. Joachim, G. Cuniberti, A nanographene disk rotating a single molecule gear on a Cu(111) surface, Nanotechnology 33 (17) (2022) 175701, http://dx.doi.org/10.1088/1361-6528/ac4b4b.